Journal of Renewable Energy and Sustainable Development (RESD) Volume 11, Issue 2, December 2025 - ISSN 2356-8569
http://dx.doi.org/10.21622/RESD.2025.11.2.1430

Received: 12 June 2025 Accepted: 20 August 2025 Published: 28 September 2025

A Model for Assessing Urban Resilience of Coastal Areas Against Natural Flooding Risk

Shady Hafez Gemaila [1], Abdullah Farouk Al-Attar [2], and Hesham Mohamed El-Barmelgy [3]

[1,2,3] Cairo University, Faculty of Urban and Regional Planning, Urban Design Department, Cairo, Egypt

hafez.s.m@furp.cu.edu.eg, abdallahfarouk@cu.edu.eg, barmelgy@staff.cu.edu.eg

Abstract

Since the beginning of the 21st century, coastal areas worldwide have witnessed an accelerated severity and high frequency of natural disasters. Although coastal areas represent 15% of the inhabited areas, they host more than 60% of the world's population. This contradiction between the high population density and the sensitive ecosystem of such areas places high pressure on resources and raises the vulnerability against risks in those areas associated with natural flooding resulting from storms and tsunamis. Consequently, there is a pressing need to understand, investigate, and address the dynamics of coastal areas. The paper aims to propose a model to assess the resilience of urban coastal areas against natural flooding risks. Employing an inductive research methodology, the parameters of both the Egyptian coastal Urbanism and the natural flooding risk are analyzed and studied to define the UT-NFR (Urban Typology due to Natural Flooding Risk) Model. The model comprises three main stages: (a) identifying the risk of community pattern, (b) identifying the risk of urban Pattern, and (c) calculating the UT-NFR index. The model is challenged by the limited methods to determine the impact of the urban environment on the natural flooding risk, adding to the existing descriptive methods for classifying urban areas in Egypt. Based on a comparative study of three international cases selected due to their compatibility with Egypt, a set of indicators to identify the parameters of Egyptian Urbanism in coastal areas is initially deduced. The final list includes 58% of the deducted indicators, which are valid to act as a proactive tool to predict the degree of urban resilience for the new Egyptian coastal developments. Additionally, the model is valid for defining the degree of resilience and detecting the deficiencies of the existing coastal development, offering effective mechanisms to enhance the ability to promote the required contingency preparations.

Index-words: *Coastal floods, Resilient Urbanism, Digital tools, Egyptian communities.*

I. Introduction with literature review

Along 440.000 km of sensitive ecosystems, coastal populations live in a state of instability due to exposure to the risk of natural disasters caused by the natural phenomena associated with seas and oceans, such as storms and tsunamis [1]. Such a vulnerable coastal population has been doubled and is still increasing to host around 60% of the world's population in areas that represent only 15% of the inhabited land worldwide [2]. The Egyptian coasts, along 1,150 km on the Mediterranean and 1,850 km on the Red Sea, are exposed to many environmental and socio-economic pressures [3]. Coasts on the Mediterranean are part of the most fragile marine regions due to faults that cause destructive tectonic activity side by side with unsustainable policies of development, especially on the Northern West Coast of Egypt [4].

Regarding the concept of sustainable development, the international community explores ways to face risks at coasts by improving resilience depending on natural, socio-economic, and strategic approaches [5], [6]. The strategic approach includes displacement plans to face long-term phenomena as sea level rise and instant evacuation plans to face short-term events as floods risks [7], [8]. These plans operate depending on routes, buildings, and outdoor spaces representing the components of the urban environment [9], [10].

Variations of urban components provide different urban configurations known as urban forms [11]. A sustainable coastal urban form should be able to adapt the uniqueness of a coastal area including natural, cultural, and social needs [11]. Several studies attempted to set a classification for the Egyptian Urbanism depending on three standards; level of Governance, socio-economic patterns, and urban patterns [12].

Copyright © 2025, authors

Volume 11, Issue 2, December 2025 - ISSN 2356-8569
http://dx.doi.org/10.21622/RESD.2025.11.2.1430

The Egyptian Urbanism needs to be re-classified in accordance with the coastal flooding risk [10]. Consequently, an inductive research method is employed to propose a framework depending on the degree of resilience for the main parameters:

a. The urban Pattern including:
   (i) urban fabric,
   (ii) urban network,

b. The community pattern including:
   (i) degree of hazard,
   (ii) vulnerability,
   (iii) resistance. (Fig.1)

This paper introduces the UT-NFR (Urban Typology due to Natural Flooding Risk) model based on the findings of a comparative study analysis for a number of cases compatible with Egyptian Urbanism. The model comprises three main stages:

a. Identifying the risk of community pattern,

b. Identifying the risk of urban Pattern,

c. Calculating the (UT-NRF) index that ranges between 0 and 1 due to the linear normalization for the included indicators for both patterns. (Fig.1)

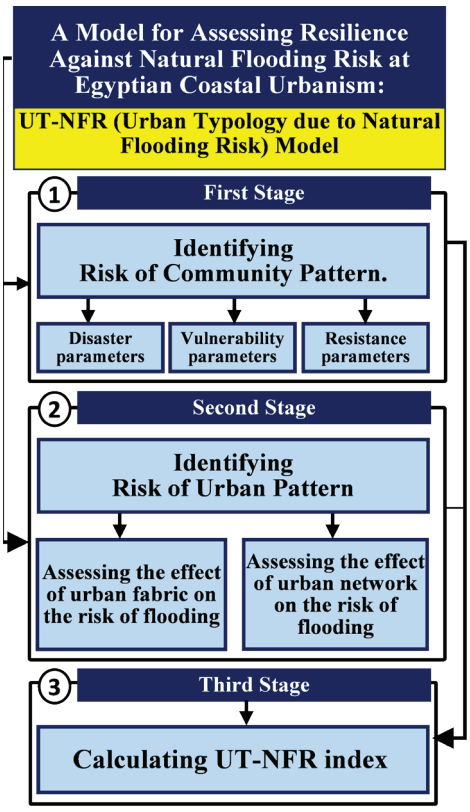


Figure 1: Proposed Framework.

A. *Natural disaster and coastal Egyptian Urbanism*

1. Natural disasters and Egyptian coasts

A disaster is an unexpected event that causes damage, human suffering, and overwhelming local capabilities [13], [14]. Disasters classified as natural, human-caused, and combined of both causes could be described by source, location, and occurrence rate [15]. The most critical hazard is global warming, which causes the sea level to rise by 1 to 2 mm annually [16]. Natural coastal disasters are classified into:

a. Long-term phenomena such as sea level rise or landslides,

b. Short-term phenomena including storms and tsunamis [17], [18].

Egypt typically faces sea level rise, tsunamis, and 26 seasonal maritime storms [19], [20]. A set of non-seasonal storms caused more than 227,000 victims and half a billion dollars in property losses in Egypt since the 1990s [21]. Historically, Egypt has been exposed to a well-documented number of tsunamis from the Mediterranean as a seismically active region, causing a major event almost every 800 years [22]. One of the events occurred in the year 365, and the second one occurred in 1303, which destroyed the ancient, significant world wonder of the Alexandria lighthouse [23], [24].

There are concerns towards the unstable geological conditions of Etna Mountain which is known for its volcanic activity at the east of the Mediterranean in a way that may cause a tsunami hitting North Africa [25]. In May 2017, researchers observed a sliding of 8 cm in Mount Etna's edge at the south of Sicily confirming the previous concerns towards it [26].

2. Existing conditions of coastal cities

While a coast refers to the area of contact between land and sea, coastal areas are the interactions between land, sea, and atmosphere [27]. The total length of the world's coastline is one million km, embracing 60% of the world's population, occupying only 40% of its accessible total length within glacial, shelf, plain, vegetated, and marine island coasts [28]. Coasts are remarkable dynamic environments containing resources for food and habitats in a highly sensitive ecosystem [29]. About 23% of the world's population occupies 100 km of the coastline, inhabited by activities such as fishing, trade, and

Volume 11, Issue 2, December 2025 - ISSN 2356-8569
http://dx.doi.org/10.21622/RESD.2025.11.2.1430

tourist activities determined by the natural and demographic composition [30]. The risk of living by coasts has escalated since the percentage of Gross Domestic Product exposed to storms increased from 3.6% in 1970 to 4.3% in the 21st century, besides increased losses of coastal habitats, which reached 85% of marine forests, 50% of wetlands, and more than 25% of coral reefs [31]. A set of demographical, socio-economic, political, and natural forces, such as population growth, urbanization, and industrialization, contributed to the aggravation of that risk [15].

A number of threats emerged on the Mediterranean coasts, such as pollution in the eastern basin and the Adriatic Sea, with the non-stop biological invasions and algal blooms due to the huge proliferation of more than 600 alien plants and animals recorded between 1970 and 1980 [32]. The Mediterranean coasts face catastrophic effects on public health due to the consumption of toxic seafood, which appears in sewage from marine navigation and agricultural discharges, in addition to the risk of natural disasters, including earthquakes, volcanoes, and tsunamis [32].

On the other hand, a number of threats have emerged along the coasts of the Red Sea such as the fluctuated tidal rates with submersion operations up to 3 km deep [32]. The widespread of coral reefs and mangrove forests along 2000 km hinders the sustainable tourism development, adding to the tectonic activity of the Great Rift Valley, and the expansion of oil pollution by mining [32].

Based on the index of coastal vulnerability, a set of influential parameters, including geomorphology, slope, exposure to erosion, sea level, and tide values, is used to classify the Egyptian North Coast. Thus, the Egyptian North Coast is divided into five sectors due to the homogeneity of these parameters [33] (Fig.2).



Figure 2: Egypt North Coast classified by vulnerability index.
(Source: prepared by the authors, based on [33])

The western sector of the Egyptian North Coast from Salloum to El-Hammam faces high erosion rates due to the modification of the shoreline to accommodate more touristic activities and the unplanned areas that exceed 70% of human settlements [4]. The second sector, between El-Hammam and Edko, is exposed to developmental pressures on resources that led to pollution and infrastructure deterioration [29].

The sector at the Delta, between Idku and Port Said, is exposed to drying of wetlands, land subsidence, and decreased sedimentation rate of the Nile, which decreased to 3.92 billion m3/year through the Rosetta Estuary in 2007 instead of 62 billion m3/year in 1912 [29].

The sector extending 70 km east of Port Said to Bardawil suffers from shoreline changes resulting from the construction of a breakwater at El-Arish power station in 1995 and El-Arish fishing port in 1982, with a rate of 35% erosion and 65% sedimentation [4]. Nonetheless, the areas extending 130 km east of Bardawil to Rafah are exposed to a rate of 70% erosion and 30% sedimentation [4]. Based on the index of vulnerability, which includes geomorphology, slope, erosion, fauna or flora coverage, and land use, a set of influential parameters is used to classify the coast of the Red Sea that could be divided into a number of sectors due to the diversity and lack of uniformity [33] (Fig.3).

Volume 11, Issue 2, December 2025 - ISSN 2356-8569
http://dx.doi.org/10.21622/RESD.2025.11.2.1430

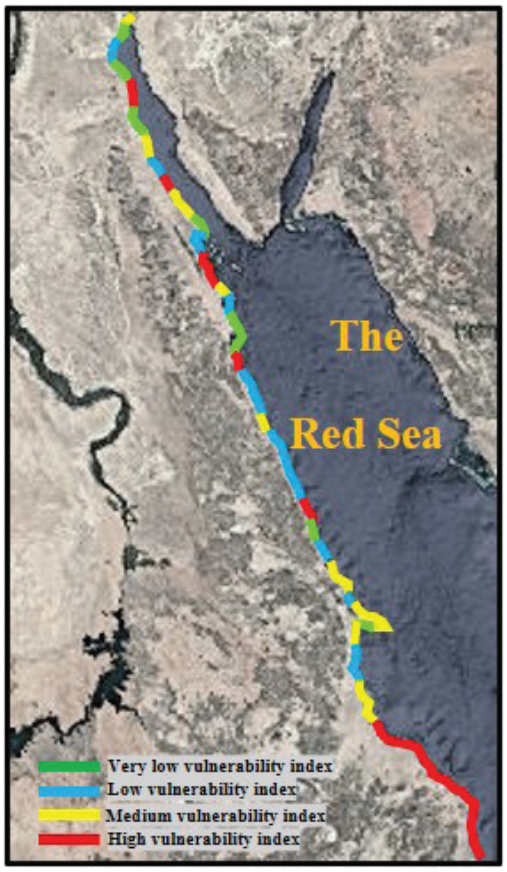


Figure 3: Egypt East Coast classified by vulnerability index.
(Source: prepared by the authors, based on [33])

3. Coastal flooding scenarios on Egyptian coasts

Coastal flooding is an inundation of coastal lands and properties, especially in areas with high population densities, resulting from storms or tsunamis with an increased impact on areas below sea level [17], [18]. Flooding is affected by a set of factors, including sea level rise and extreme weather events [34]. The degree of risk is differently affected by demographic, economic, environmental, and urban characteristics [35]. As different types of beach geomorphology record different response patterns to flooding, the impact of coastal flooding depends on the level of vulnerability, sensitivity, and resistance [36].

In addition to seasonal typical storms on the Egyptian coasts, non-seasonal events from storms or tsunamis on the Northern Coasts have historically caused more than 227,000 victims and more than half a billion dollars loss of properties [22]. In the future, Egypt is expected to face a possible hurricane at the eastern basin of the Mediterranean, especially after the disaster of Derna, Libya in 2023 [37].



Figure 4: Etna Mountain and Egyptian North Coast.
(Source: prepared by the authors, based on [25])

The geological conditions of Sicily, especially Mount Etna, signal a possible future tsunami to hit the coasts of North Africa [25] (Fig. 4). Based on history and existing geological conditions, the risk of a tsunami is limited to the Egyptian North Coast [22]. Thus, the Egyptian North Coast is divided into four sectors, which discuss the worst scenarios of a tsunami [38], [39]. All sectors are subjected to the tsunami scenario of the year 1303, while the worst scenario likely to affect the sector along the Delta is the tsunami scenario of 365 [10] (Fig. 5).

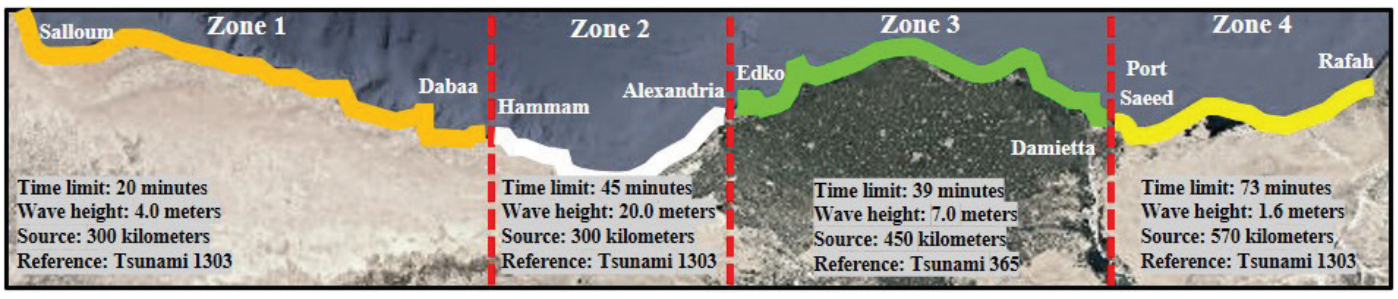


Figure 5: Future scenarios of tsunamis. Tsunami on the Egyptian North Coast.
(Source: prepared by the authors, based on [22], [38], [39])

http://dx.doi.org/10.21622/RESD.2025.11.2.1430

4. Urban resilience at coasts and flooding risk: Approaches and strategies

Sustainability in coastal areas can be measured through the ability to face the forces of flooding, adapt to them, and restore stability to perform functions in a process called urban resilience [40], [41]. While urban community is the material exposed to forces, urban resilience could be defined as the ability to absorb forces with flexible releasing due to the qualities of resistance, balance, and cohesion that could be achieved depending on three main approaches:

a. The environmental approach,

b. The socio-economic approach,

c. The strategic planning approach [42].

The environmental approach appears through the coastal resources management policy, which depends on preserving resources and reducing the destructive forces of flooding [40], [43]. This policy relies on coastal forests, mangroves, dunes, and coral reefs certified to reduce up to (40-50) % of the destructive effects in Southeast Asia during the 2004, 2006, and 2007 tsunamis [44].

The socio-economic approach appears through a set of social policies such as raising awareness, encouraging participation, placemaking for open spaces depending on user well-being strategies, and training teams of emergency support [15], [45]. This aligns with set of economic policies such as conservation, development, and creating interactions with economic basis [46].

The strategic planning approach appears through the urban disaster management strategy, aiming to achieve a high response to risk and mitigate the destructive effects of coastal flooding through two main groups of policies [47], [48]. The first is a group of urban policies including safe use allocation, fortified landscaping, upgrading, replacement, renewal plans, improving infrastructure, and waterfront development [49], [50]. The second is a group of organizational policies, including displacement plans to deal with long-term phenomena such as rising sea level and evacuation plans to deal with short-term phenomena such as storms and tsunamis [51]. The evacuation is the process of moving people to safe areas to reduce potential losses by the involved parties [51]. However, the individual responsibility to survive is a main motive; parallel preparations for the disadvantaged groups are required to overcome the mobility inequality in densely populated cities [52], [53].

Evacuation operations consist of warning systems, signage systems, and escape maps that depend on buildings for vertical evacuation, urban spaces for horizontal evacuation, escape routes on streets, service centers for rescue preparations, and districts as hazard zones [54], [55], [45]. This highlighting the role of the urban environment to achieve sustainability of the coastal areas [56], [57].

5. Egyptian Urbanism: Typological forms and patterns

The role of the urban environment to achieve sustainability at the coastal areas have been proven through activating strategies such as evacuation plans [58], [59], [60]. Sustainable Urbanism depends on a sustainable urban form that needs to be raised in consistency with the parameters of an urban area, especially areas of a high sensitivity index such as coastal areas facing the natural flooding risk [61], [62].

An urban form is defined as a product of the accumulation of the city over time in a spatial space [11]. This accumulation is created by masses suitable for life purposes explaining the ability of urbanization to meet needs of confronting flooding risk and reduce the losses caused by the deficiency of these urban forms [63]. Several studies have indicated that different patterns of urban forms had been crystalized according to a set of parameters of different sectors in a process known as the typology of urban form [64].

The Egyptian Urbanism is classified based on the method of triple typology for urban forms, which contributed to a deep understanding of these complicated systems with three bases, including:

a. Urban Governance,

b. Community pattern,

c. Urban Pattern [12].

The base of urban Governance represents the level of controlling and organizing the urban morphology through three main indicators, including spontaneous, semi-organized, and organized levels [12]. The base of community pattern expresses the nature of relationships between residents

http://dx.doi.org/10.21622/RESD.2025.11.2.1430

through three main indicators, including Bedouin, rural, and urban patterns [12]. The base of urban Pattern emerged by vertically-built volumes with horizontally-extended spaces consisting of two basic elements:

a. Urban fabric issuing the principles of densities, clustering, and ordering with outputs of compacted, integrated, loose, and scattered urban fabrics,

b. Urban network issuing the shape of circulation system with outputs of primitive, grid, and collective systems [12].

The possibility of having patterns for urban forms based on the method of triple typology produces unrealistic patterns, such as coupling the Bedouin pattern with an organizational level of Governance and an integrated urban fabric [12]. Additionally, a number of patterns expressing the predominant logic of urban forms are produced [12] (Fig. 6).

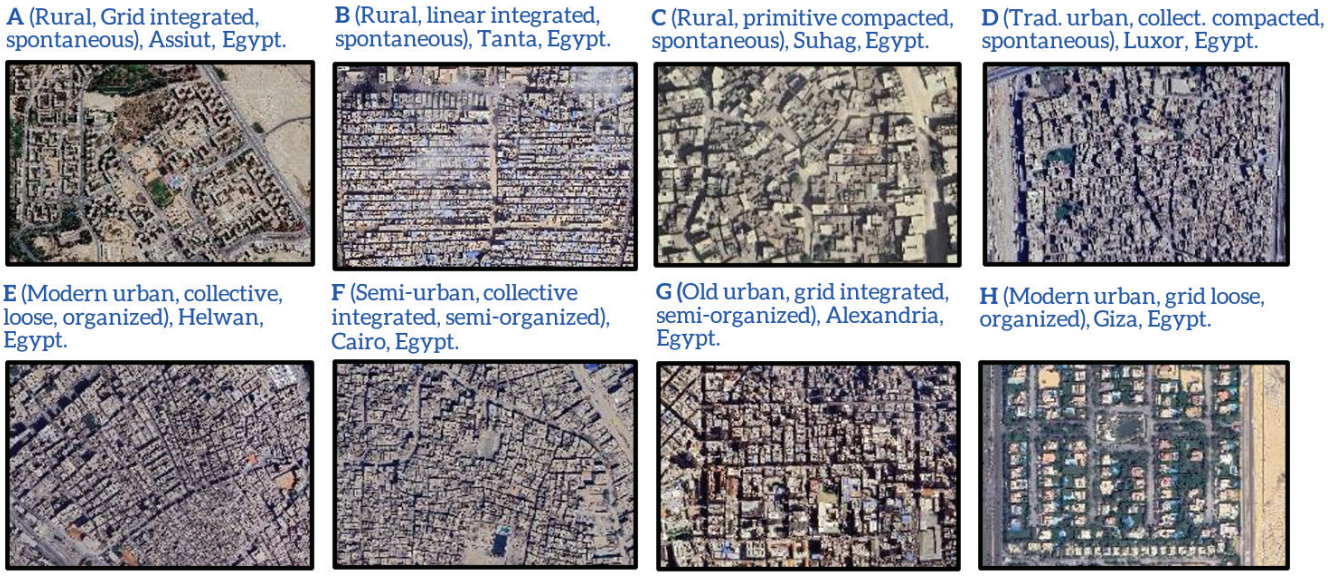


Figure 6: Examples of the predominant patterns of urban forms in Egypt.
(Source: prepared by the authors, based on [12])

Based on the method of triple typology for the urban form of Egypt, the predominant patterns of urban form along the Egyptian coasts and their recurrence rate are identified using samples from the North Coast [10], [12] (Fig. 7).

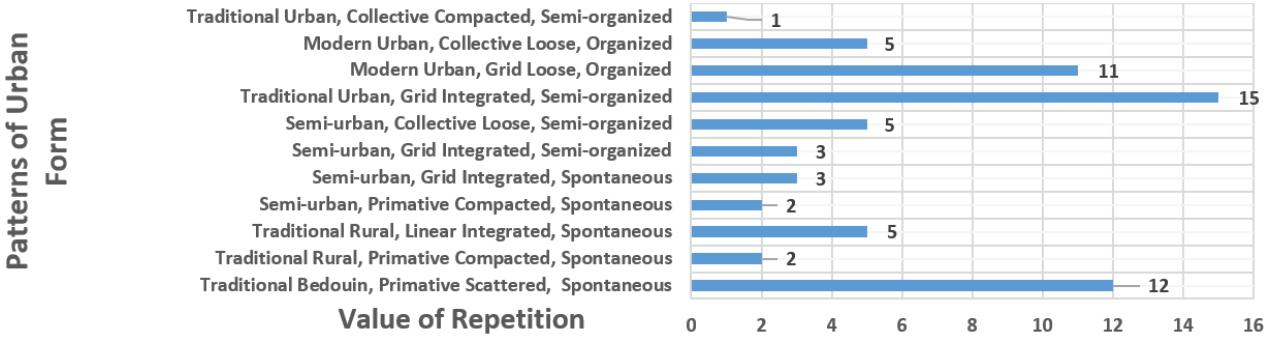


Figure 7: Prevailing patterns of urban form at the Egyptian North Coast and the rate of repetition.
(Source: prepared by the authors, based on [10])

B. Case studies of digital models for urban resilience in coastal areas

Recent research on coastal sustainability in Egypt demonstrated that indicator-based models are the most practical tools to integrate urban parameters with natural risk considerations [65]. Among the set of global models measuring urban resilience at coastal areas, three models are selected based on proposed evaluation criteria to investigate the most appropriate models matching the Egyptian coastal Urbanism (Table 1), and (Fig. 8).

http://dx.doi.org/10.21622/RESD.2025.11.2.1430

Table 1: List of initial global models, with color code, and final score

Code	List of initial global models	Score
1	MAS-Based Evacuation Simulation of an Urban Community during an Urban Rainstorm Disaster in China [66].	6.60
2	Hurricane Evacuation Modeling Using Behavior Models and Scenario-Driven Agent-based Simulations [67].	5.70
3	Modeling Evacuation Behavior Under Hurricane Conditions [68].	5.50
4	**The Impact of Urban Form Facing Risk of Tsunami** [10].	8.10
5	Quantitative analysis of urban form: a multidisciplinary review [69].	5.10
6	**Urban Form and Natural Hazards: Exploring the Dual Aspect Concept of Urban Forms on Flood Damage** [70].	7.50
7	**Coasts at Risk: An Assessment of Coastal Risks** [71].	7.60
8	Coastal Hazard Vulnerability Assessment Based on Geomorphic, Oceanographic, and Demographic Parameters [72].	5.70
9	Mapping Urban Resilience for Spatial Planning [73].	6.70
10	An interdisciplinary and catchment approach to enhancing urban flood resilience [74].	6.90

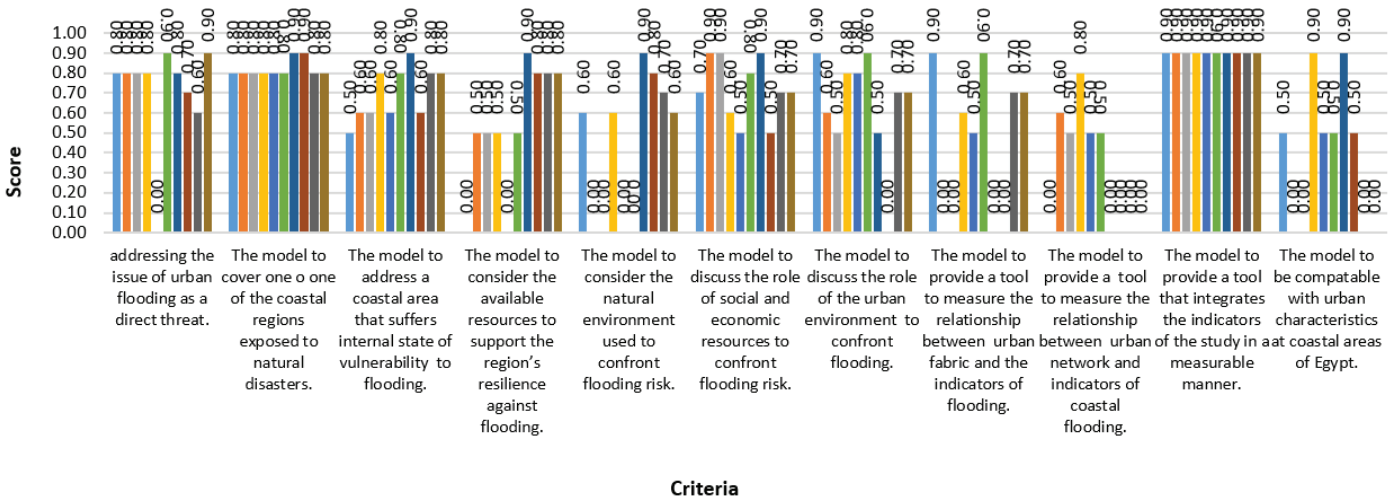


Figure 8: Evaluation criteria and score for the initial list of global models for urban resilience at coastal areas.

Based on the evaluation criteria for the initial list of global models, the most suitable practices are numbers 4, 6, and 7, respectively. These practices will be used to develop a deeper understanding of the relation between formative parameters of Egyptian coastal Urbanism and natural flooding risk, and develop the proposed model for assessing urban resilience against the risk of coastal flooding.

The evaluation process assigned numerical values to indicate the suitability of each model to the thesis, with a minimum score of 0.5 expressing a descriptive adherence to the criteria, without having tools or final results to prevent value dispersion from ineffective scores. Three categories are defined for the evaluation, including (>0.5 to 0.7) for tools without results, (>0.7 to 0.9) for tested tools with expressive results, and (>0.9 to 1) for validated tools.

1. Role of urban network facing risk of Tsunami: A case of Egyptian North Coast

Based on formative parameters of urban fabrics, the evacuation plans will be used to identify the risk of the urban network along the Egyptian North Coast employing a model to predict the survival rates generated by GIS [10], [75] (Table 2), and (Fig. 9).

http://dx.doi.org/10.21622/RESD.2025.11.2.1430

Table 2: Results of the application of evacuation plans on areas exposed to flooding along the Egyptian North Coast
(Source: prepared by the authors, based on [10], [75])

Urban fabric	Temporal Surviving Population				Accumulative Surviving Population				Survival Rate			
	First (5) minutes	Second (5) minutes	Third (5) minutes	Fourth (5) minutes	After (5) minutes	After (10) minutes	After (15) minutes	After (20) minutes	After (5) minutes	After (10) minutes	After (15) minutes	After (20) minutes
Primitive Compacted	58334	41178	32221	32221	58334	99512	131733	163954	26%	44%	59%	73%
Linear Integrated	59647	54831	48946	44367	59647	114478	163424	207791	27%	51%	73%	92%
Grid Integrated	59982	42876	39257	35900	59982	102858	142115	178015	27%	46%	63%	79%
Grid Loose	60003	48176	45575	36258	60003	108179	153754	190012	27%	48%	68%	84%
Collective Loose	62513	57000	54393	51033	62513	119513	173906	224939	28%	53%	77%	100%

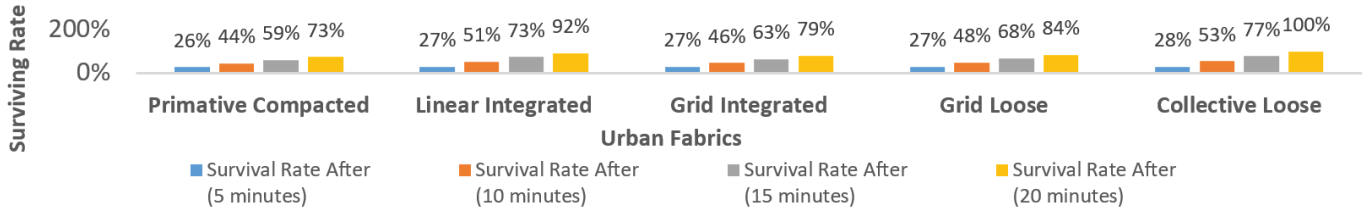


Figure 9: Results of the application of evacuation plans on areas exposed to flooding along the Egyptian North Coast. (Source: prepared by the authors, based on [10], [75])

The most remarkable output is that linear integrated fabric offers a 92% survival rate despite its high densities. This comes as a result of its perpendicular network on the shoreline, facilitating evacuation by minimizing the routing length and time needed to reach shelters [10].

2. Impact of urban form on flooding risk: A case of Seoul, South Korea

A set of factors is utilized to describe an urban form in the area affected by flood damage in the case of Seoul, South Korea, including Floor Area Ratio, which increases directly with the increased flood damage [70]. However, Population Density, Urban Dispersion depending on the Gini coefficient, Urban Clustering depending on Moran's I index, and Randomness (irregularity) of Spatial Distribution depending on the Entropy Index increase inversely with the increase of flood damage [70].

3. Assessing community risk at coasts: A global assessment of the case of flooding

The index of coastal risk expressing resilience against coastal flooding is calculated by combining indicators, including exposure, vulnerability, and resistance [71]. This method is used to calculate the risk of community pattern in the equation $CR = D \times \left(\frac{V \pm A}{2}\right)$, where $\boldsymbol{CR}$ is the index of coastal risk due to community pattern, while $\boldsymbol{D}$ is the degree of exposure, $\boldsymbol{V}$ is the degree of vulnerability, and $\boldsymbol{A}$ is the degree of Adaptability that equally represents resistance.

II. Methodology

A. Urban Typology due to Natural Flooding Risk UT-NFR Model

UT-NFR is a proposed model to measure urban resilience against coastal flooding at the Egyptian coastal Urbanism, depending on calculating the risk of its two main parameters. The first parameter is the community pattern developed by combining: (A) the level of urban governance, and (B) the type of socio-economic Pattern. The second parameter is the urban Pattern, developed by keeping its both original components: (C.1) urban fabric, and (C.2) urban network, which were traditionally proposed to classify Egyptian Urbanism throughout several previous studies. UT-NFR index ranges between (0) and (1) due to the process of linear normalization for the included indicators that describe Egyptian coastal Urbanism (Fig. 10).

http://dx.doi.org/10.21622/RESD.2025.11.2.1430

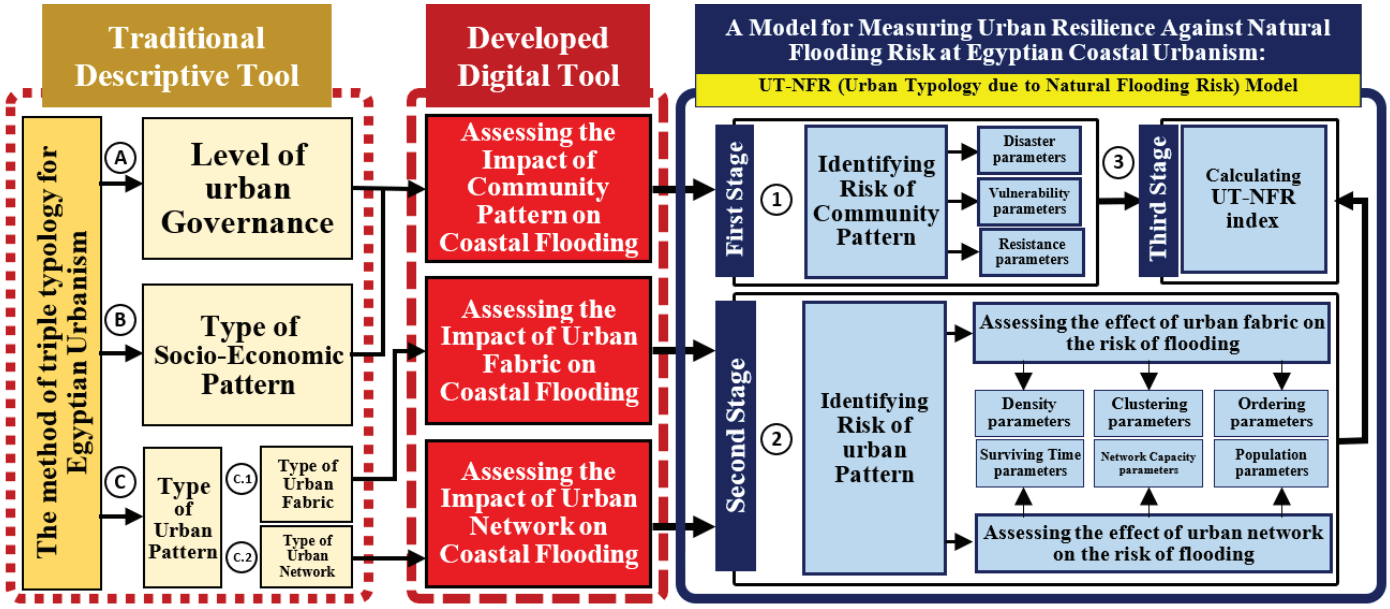


Figure 10: A theoretical framework for the UT-NFR model.

1. Stage 1: Identifying the risk of the community pattern parameter

This parameter relies on measuring natural, socio-economic, and governance indicators to assess three main principles:

a. Hazard,

b. Vulnerability,

c. Resistance employing a set of validated indicators [71], as indicated in Eq. (1):

$$CP_i = \left(\left[\frac{\sum(H_n \times W_h)}{\sum W_h} \times H_{if}\right] + \left[\frac{\sum(V_n \times W_v)}{\sum W_v} \times V_{if}\right]\right) \div \left(\frac{\sum(R_n \times W_r)}{\sum W_r} \times R_{if}\right) \times \frac{1}{\sum if} \quad (1)$$

Where CP_i is the main risk parameter of community pattern, H_n is the linear-normalized value for an indicator of hazard in an area, W_h is the relative weight of this indicator, and H_{if} is the impact factor for the hazard principle. V_n is the linear-normalized value for an indicator of vulnerability in an area, W_v is the relative weight of this indicator, and V_{if} is the impact factor for the vulnerability principle. R_n is the linear-normalized value for an indicator of resistance in an area, W_r is the relative weight of this indicator, and R_{if} is the impact factor for the resistance principle. Linear-normalized values for principles of hazard, vulnerability, and resistance [71] are indicated in Eq. (1-1):

$$X_n = \frac{X_0 - X_{min.}}{X_{max.} - X_{min.}} \quad (1\text{-}1)$$

Where X_n is the linear-normalized value for an indicator, X_0 is the actual value of this indicator in an area, $X_{min.}$ is the minimum officially-recorded value of the indicator historically, and, $X_{max.}$ is the maximum officially-recorded value of the same indicator historically.

2. Stage 2: Identifying the risk of the urban pattern parameter

This parameter relies on measuring the urban form impact on flooding by assessing two principles:

a. The impact of urban fabric on flood losses,

b. The impact of urban network on survival rate of evacuees during the evacuation, [70], as indicated in Eq. (2):

$$UP_i = \left(\frac{L_0 - L_{min.}}{L_{max.} - L_{min.}} \times UF_{if}\right) \div \left(P_t \times \frac{\sum([T_b \times P_b] + [T_s \times P_s])}{N_{areas}} \times \left[\frac{1}{T_m}\right] \times UN_{if}\right) \times \frac{1}{\sum if} \quad (2)$$

Where UP_i is the main risk parameter of urban Pattern, L_0 is the predicted value of flooding losses in an area, $L_{min.}$ and L_{max} is the minimum and maximum officially recorded historical values of flooding losses, respectively. P_t is the total population of an urban

http://dx.doi.org/10.21622/RESD.2025.11.2.1430

area, T_b and T_s are the required time to evacuate a building and to arrive at a safe assembly area on the urban network at the sub-area, respectively, P_b and P_s are estimated proportions of the population inside buildings and on streets, respectively. N is the total number of module areas, and T_m is the allowed time to complete the evacuation plan. UF_{if} and UN_{if} are the impact factors for the urban fabric and the urban network principles, respectively [10], [70], [75].

- ***Step 1: Assessing the effect of urban fabric on flooding risk***

  The study adopts a numerical tool to assess the impact of engineering characteristics of an urban fabric on flooding losses [70], as indicated in Eq. (2-1):

$$\boldsymbol{L_0} = \left(\left[\frac{(\partial + FAR_i + \cdots)}{(D_i + G_i + M_i + E_i + \cdots)}\right] + \left[1 - \frac{\partial - \sum(\boldsymbol{\mu_i})}{\partial}\right]\right) \times \frac{1}{\sum i} \quad (2\text{-}1)$$

  Where ∂ is the coefficient for the average value of historical flood losses in official records, FAR_i is the floor area ratio, D_i is the population density, G_i is the Gini coefficient referring to the degree of urban dispersion, M_i is Moran's I index referring to the degree of urban clustering, and E_i is the Entropy index referring to the degree of urban distribution. $\boldsymbol{\mu_i}$ is the indicator that has an impact on losses to calculate Mean Absolute Error, and $\boldsymbol{i}$ is the impact factor for an indicator.

- ***Step 2: Assessing the effect of urban network on flooding risk***

  Recent studies prioritize pedestrian mobility during the evacuation of densely populated cities to avoid congestion caused by high traffic demand. This promotes walkability through improving the morphological, functional, and social dimensions [76].

  The study adopts a numerical tool to simulate the evacuation process using pedestrian routes as a priority to assess the impact of urban network characteristics on the survival rate. This tool is carried out using the Pedestrian Evacuation Analyst as a GIS application. Meanwhile, Global Mapper is utilized to obtain geospatial data to get the inundation maps of the potential flooding scenario [10], [75]. The required time to evacuate a building to a safe location on the urban network is indicated in Eq. (2-2-A) and Eq. (2-2-B):

$$\boldsymbol{T_b} = \frac{4\sqrt{\boldsymbol{A_{unit}}} + \boldsymbol{F_{avg}}(\boldsymbol{\beta} + \boldsymbol{B_{depth}})}{(\boldsymbol{\delta_0} \times [1 + iBF_x] \times [1 - iBF_y] \times \cdots)} \quad (2\text{-}2\text{-A})$$

$$\boldsymbol{T_s} = \frac{(\boldsymbol{S_{avg}} + \boldsymbol{R_{eva}}) \times \boldsymbol{\lambda}}{(\boldsymbol{\alpha_0} \times [1 + iBF_x] \times [1 - iBF_y] \times \cdots)} \quad (2\text{-}2\text{-B})$$

  Where $\boldsymbol{A_{unit}}$ is the average area of a unit as per the maximum perimeter distance to exit unit, $\boldsymbol{F_{avg}}$ is the average number of floors, $\boldsymbol{\beta}$ is a constant coefficient due to the typical height of floor for the distance on stairs, and $\boldsymbol{B_{depth}}$ is the block depth for the distance on internal corridors of a building. $\boldsymbol{S_{avg}}$ is the average length of the internal evacuation route at a module area, $\boldsymbol{R_{eva}}$ is the length of the horizontal evacuation route on the main external urban network, and $\boldsymbol{\lambda}$ is the Spatial Deviation Coefficient between theoretical and physical distances. $\boldsymbol{\delta_0}$ is the average speed for the prevailing age category of residents, iBF_x and iBF_y are variables that have a positive or negative impact on the evacuation speed [10], [75].

3. Stage 3: Calculating the UT-NFR index

Finally, UT-NFR is calculated based on the main risk parameters of the community and the urban patterns [71], [70], [75], as indicated in Eq. (3):

$$\boldsymbol{UT - NFR} = \left(\frac{\sum i}{iCR_i + iUP_i}\right) \quad (3)$$

Where $\boldsymbol{CR_i}$ is the risk of the community pattern parameter, $\boldsymbol{UP_i}$ is the risk of the urban pattern parameter, and $\boldsymbol{i}$ is the impact factor for parameters.

B. Adaptation of the UT-NFR Model within the Egyptian context

A set of indicators was developed to apply the proposed UT-NFR model to the Egyptian context based on a deep understanding of Egyptian Urbanism. Each indicator's relative weight is determined through a comparative study, highlighting the degree of each global model reliance on each indicator in Tables (3, 4, 5, 6, and 7), while (M1), (M2), and (M3) are the given reliance evaluation for the global models included into the previously selected case studies numbers (4, 6, and 7) respectively, as follows:

http://dx.doi.org/10.21622/RESD.2025.11.2.1430

Table 3: Indicators for the level of hazard to identify the risk of community pattern with relative weights
(Source: prepared by the authors, based on [71])

Indicator		Principle	Relative Weight			
			M1	M2	M3	Final Score
Level of Hazard	H1	Rainfall rate in the region during the coastal storm season.	4	5	4	4.33
	H2	Rainfall rate in climate exceptions caused by cyclones.	2	2	3	2.33
	H3	Blizzard rate during the coastal cyclone season.	1	1	3	1.67
	H4	Thunderstorm rate during the coastal cyclone season.	1	1	3	1.67
	H5	The temperature rate drops to zero or below during the coastal cyclone season.	1	1	3	1.67
	H6	Average number of consecutive days that a coastal cyclone lasts.	1	1	3	1.67
	H7	Average wave height during the coastal cyclone season.	2	1	4	2.33
	H8	Average prevailing wind speed during the coastal cyclone season.	1	1	3	1.67
	H9	Historical temporal sequence of tsunami occurrence.	4	1	3	2.67
	H10	Average wave height of the Tsunami.	4	2	4	3.33
	H11	Average wave Speed of Tsunami.	2	1	3	2.00

Table 4: Indicators for the level of vulnerability to identify the risk of community pattern with relative weights
(Source: prepared by the authors, based on [71])

Indicator		Principle	Relative Weight			
			M1	M2	M3	Final Score
Level of Vulnerability	V1	The rate of coastal erosion.	1	1	3	1.67
	V2	The rate of pollution of the regional seawater.	1	1	3	1.67
	V3	The rate of air pollution.	1	1	3	1.67
	V4	The rate of salinity of the regional water.	1	1	3	1.67
	V5	The rate of oil spills observed in the regional seawater.	1	1	3	1.67
	V6	The percentage of land below sea level.	2	2	3	2.33
	V7	The announced unemployment rate.	1	4	3	2.67
	V8	The announced dependency ratio.	1	4	3	2.67
	V9	The outbreak rate of chronic diseases.	2	1	3	2.00
	V10	The outbreak rate of infectious diseases and epidemics.	2	1	3	2.00
	V11	The percentage of children.	3	1	3	2.33
	V12	The percentage of elderly people.	3	1	3	2.33
	V13	The percentage of handicaps.	3	1	3	2.33
	V14	The percentage of families that raise pets.	2	1	3	2.00
	V15	The percentage of accommodations in mental hospitals.	2	1	3	2.00
	V16	The percentage of prisoners.	2	1	3	2.00
	V17	The percentage of workers in public and basic services.	2	1	3	2.00
	V18	The percentage of families that do not have emergency and evacuation equipment.	3	1	3	2.33
	V19	The percentage of residents without a training session on evacuation.	2	1	3	2.00
	V20	The percentage of land not suitable for development.	2	2	3	2.33
	V21	The percentage of families below the poverty line.	2	2	3	2.33
	V22	The percentage of families that do not own private cars.	2	1	3	2.00

http://dx.doi.org/10.21622/RESD.2025.11.2.1430

Level of Vulnerability	V23	The percentage of families that depend on self-employment or non-stable crafts.	1	2	3	2.00
	V24	The percentage of families having income from coastal resources.	1	1	3	1.67
	V25	The percentage of the gross domestic product based on coastal activities.	1	1	3	1.67
	V26	The percentage of streets less than 14m wide out of the total number of streets.	2	1	3	2.00
	V27	The percentage of unpaved streets.	4	1	2	2.33
	V28	The percentage of streets without evacuation lanes.	4	1	2	2.33
	V29	The percentage of residential units located on ground floors.	2	1	3	2.00
	V30	The percentage of buildings with a height of less than three floors.	2	1	3	2.00
	V31	The percentage of non-concrete buildings.	2	1	3	2.00
	V32	The percentage of buildings with weak structural conditions.	2	1	3	2.00
	V33	The percentage of buildings that do not contain a vertical evacuation shelter.	2	1	3	2.00
	V34	The percentage of areas not supported by warning systems.	2	1	3	2.00
	V35	The percentage of areas not supported by escape guidance signs.	2	1	3	2.00
	V36	The percentage of areas outside the coverage zones of rescue centers.	2	1	1	1.33
	V37	The percentage of areas outside the coverage scope of services.	2	1	1	1.33
	V38	The percentage of areas without escape plans.	2	1	3	2.00
	V39	The average distance between residential buildings and the nearest rescue center.	2	1	1	1.33
	V40	The average walking distance between residential buildings and the nearest shelter.	2	1	1	1.33

Table 5: Indicators for the level of resistance to identify the risk of community pattern with relative weights
(Source: prepared by the authors, based on [71])

Indicator		Principle	Relative Weight			
			M1	M2	M3	Final Score
Level of Resistance	R1	The percentage of coastal front length covered by coral reefs.	2	1	4	2.33
	R2	The ratio of the depth of coral reefs to the depth of the area.	2	1	1	1.33
	R3	The percentage of the coastal front covered by mangrove.	2	1	4	2.33
	R4	The ratio of the mangrove's depth to the depth of the area.	2	1	1	1.33
	R5	The ratio of the mangrove average height to the height of the flood.	2	1	1	1.33
	R6	The percentage of the area covered by dunes and sand grasses.	2	1	3	2.00
	R7	The ratio of dunes and sand grass average height to the height of floods.	2	1	1	1.33
	R8	The percentage of area covered by coastal forests.	2	1	4	2.33
	R9	The ratio of the average height of trees to the average height of floods.	1	1	1	1.00
	R10	The percentage of the area located above sea level.	2	1	4	2.33
	R11	The ratio of land and building volumes above sea level to flood water volume.	1	1	1	1.00
	R12	The prevailing average of the crossing slope at the shoreline.	3	1	2	2.00
	R13	The ratio of vacant housing units to the total housing units.	1	1	2	1.33
	R14	The percentage of the population (from 21 to 40 years).	2	2	3	2.33
	R15	The ratio of the working population to the total population at working age.	2	2	3	2.33
	R16	The ratio of training hours on awareness against floods to total school hours.	2	1	2	1.67
	R17	The ratio of hours specified for awareness against flood to total media hours.	2	1	2	1.67
	R18	The ratio of the population owning a smart device to the total population.	2	1	2	1.67
	R19	The percentage of the population using warning applications related to flood risks.	2	1	2	1.67
	R20	The percentage of workers at the agencies responsible for monitoring floods of the total workers.	2	1	4	2.33

http://dx.doi.org/10.21622/RESD.2025.11.2.1430

Level of Resistance	**R21**	The percentage of awareness and rescue volunteers out of the total population.	2	1	4	**2.33**
	R22	The percentage of families that own emergency equipment.	2	1	2	**1.67**
	R23	The percentage of families that have been trained at least once on evacuation.	2	1	2	**1.67**
	R24	The percentage of vacant lands suitable for development.	2	1	2	**1.67**
	R25	The percentage of families that receive the minimum wage (at least or above).	2	1	3	**2.00**
	R26	The percentage of families that own at least a private car.	2	1	2	**1.67**
	R27	The percentage of families whose heads depend on permanent or stable work.	2	1	2	**1.67**
	R28	The percentage of areas that have conservation plans.	2	1	3	**2.00**
	R29	The percentage of families that don't depend on coastal resources.	2	1	2	**1.67**
	R30	The percentage of GDP based on non-coastal activities.	2	1	3	**2.00**
	R31	The percentage of areas that are not exposed to risks.	2	1	4	**2.33**
	R32	The percentage of areas that are located within the scope of emergency services.	2	1	2	**1.67**
	R33	The percentage of street lengths is not less than 14 meters wide.	2	1	2	**1.67**
	R34	The percentage of paved streets.	2	1	3	**2.00**
	R35	The percentage of paved streets out of the total length of pedestrian streets.	2	1	2	**1.67**
	R36	The percentage of streets with lanes designated for emergency use.	2	1	3	**2.00**
	R37	The percentage of streets with max. Longitudinal slope is 5% of the total streets.	3	1	2	**2.00**
	R38	The percentage of streets with max. The longitudinal slope is 8% of the total number of pedestrian streets.	3	1	2	**2.00**
	R39	The percentage of streets with max. Longitudinal slope is 8% of the total non-motorized streets.	2	1	2	**1.67**
	R40	The percentage of streets with max. Longitudinal slope is 10% of the total motorized streets.	3	1	2	**2.00**
	R41	The percentage of buildings without residential units on the ground floor.	3	1	2	**2.00**
	R42	The percentage of built areas without residential use.	2	1	2	**1.67**
	R43	The percentage of buildings with more than three floors out of the total buildings.	2	1	2	**1.67**
	R44	The percentage of concrete buildings.	2	1	3	**2.00**
	R45	The percentage of buildings with medium to excellent structural condition.	2	1	3	**2.00**
	R46	The percentage of fortified lands against flood risk.	2	1	2	**1.67**
	R47	The percentage of buildings designed as per the requirements of civil defense.	2	1	2	**1.67**
	R48	The percentage of areas that have urban upgrading plans.	2	1	2	**1.67**
	R49	The percentage of land suitable for absorbing displacement and resettlement plans.	2	1	2	**1.67**
	R50	The percentage of street length covered by the storm network.	2	1	4	**2.33**
	R51	The percentage of rainwater that can be recycled.	2	1	4	**2.33**
	R52	The percentage of areas covered with smart coastal systems.	2	1	2	**1.67**
	R53	The percentage of prone areas without the need for displacement plans.	2	1	3	**2.00**
	R54	The percentage of areas supported by signs and escape signs.	2	1	3	**2.00**
	R55	The percentage of prone areas within the coverage of rescue centers.	2	1	3	**2.00**
	R56	The percentage of areas that have officially approved escape maps.	2	1	3	**2.00**

http://dx.doi.org/10.21622/RESD.2025.11.2.1430

Table 6: Indicators for assessing the impact of urban networks to identify the risk of urban Patterns with relative weights
(Source: prepared by the authors, based on [10], [75])

Indicator		Principle	Relative Weight			
			M1	M2	M3	Final Score
Impact of Urban Network	N1	The percentage of evacuation routes out of the total corridors.	3	1	2	2.00
	N2	The percentage of routes with evacuation lanes out of total routes.	3	1	2	2.00
	N3	The percentage of pedestrian routes out of total routes.	2	1	1	1.33
	N4	The percentage of routes with different patterns of movement out of the total routes.	2	1	1	1.33
	N5	The percentage of routes with movement in both directions out of the total routes.	2	1	1	1.33
	N6	The percentage of routes that are wider than 14 meters out of the total routes.	3	1	1	1.67
	N7	The percentage of straight routes that have break points out of the total routes.	1	1	1	1.00
	N8	The percentage of routes that contain more than a break point out of the total routes.	1	1	1	1.00
	N9	The percentage of routes with horizontal curves out of the total routes.	1	1	1	1.00
	N10	The percentage of routes with horizontal curves with 20m min. Radius out of total routes.	1	1	1	1.00
	N11	The percentage of pedestrian routes with max. Longitudinal slope is 8% of the total routes.	4	1	1	2.00
	N12	The percentage of routes paved with non-slip materials out of the total routes.	2	1	1	1.33
	N13	The percentage of routes supported by warning systems out of the total routes.	4	1	1	2.00
	N14	The percentage of routes supported by signage systems out of total routes.	4	1	1	2.00

Table 7: Indicators for assessing the impact of urban fabric to identify the risk of urban Pattern with relative weights
(Source: prepared by the authors, based on [70])

Indicator		Principle	Relative Weight			
			M1	M2	M3	Final Score
Impact of Urban Fabric	F1	Floor Area Ratio.	4	5	1	3.33
	F2	The percentage of residential use.	4	5	1	3.33
	F3	Population Density.	4	5	4	4.33
	F4	Degree of Urban Dispersion.	2	5	1	2.67
	F5	Degree of Urban Clustering.	2	5	1	2.67
	F6	Degree of Randomness for the horizontal configuration.	2	5	1	2.67
	F7	The percentage of the homogeneous sub-zone average area to the total area.	2	2	1	1.67
	F8	Buildings Foot Print	3	3	1	2.33

The evaluation criteria assigned a scoring scale (1 to 5) to indicate the level of reliance on each indicator as: (1) for no reliance, (2) for descriptive or indirect underlying reliance, (3) for measurable reliance, (4) for numerical reliance using a tested tool, and (5) for numerical reliance with generalized results. The study applies an equal impact factor for all principles, including hazard, vulnerability, resistance, urban fabric, and urban network. This application resulted in a 60% impact for the risk of community pattern, and a 40% impact for the risk of urban pattern parameters of the UT-NFR model.

III. Results

Determining the impact of parameters and principles and incorporating the relative weight of the crystallized indicators within the UT-NFR model led to the following set of results:

Volume 11, Issue 2, December 2025 - ISSN 2356-8569
http://dx.doi.org/10.21622/RESD.2025.11.2.1430

1. The model's main parameters, (i) risk of community pattern and (ii) risk of urban Pattern, are inversely related to the UT-NFR index, which has different impact factors (Fig. 11).

2. Model's main parameter to identify the risk of community pattern includes: (A) hazard, and (B) vulnerability principles directly related with the main parameter, while the principle of (C) resistance is inversely related with it (Fig. 11).

3. The model's main parameter to identify the risk of urban patterns includes principles: (D) the effect of urban fabric on flooding losses, directly related to the main parameter, and (E) the effect of urban network on survival rate during the evacuation process, inversely related to it (Fig. 11).

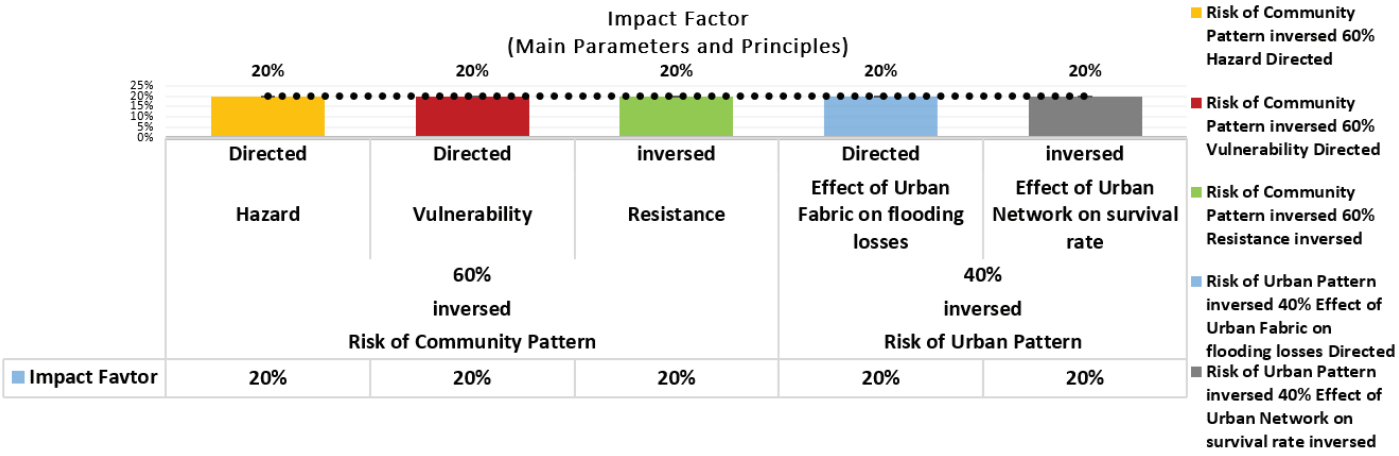


Figure 11: Main parameters and principles of the UT-NFR model and their impact factors.

4. The Arithmetic Mean of the final score is (1.95), which is very close to the value of (2), which was originally assigned for the lowest degree of reliance on indicators through the comparative study, making it the minimum acceptable value to select the valid indicators of the proposed UT-NFR model. In this context, 54 out of 129 indicators (42%), as shaded in Tables 3, 4, 5, 6, and 7 (Fig. 12), are supposed to be removed.

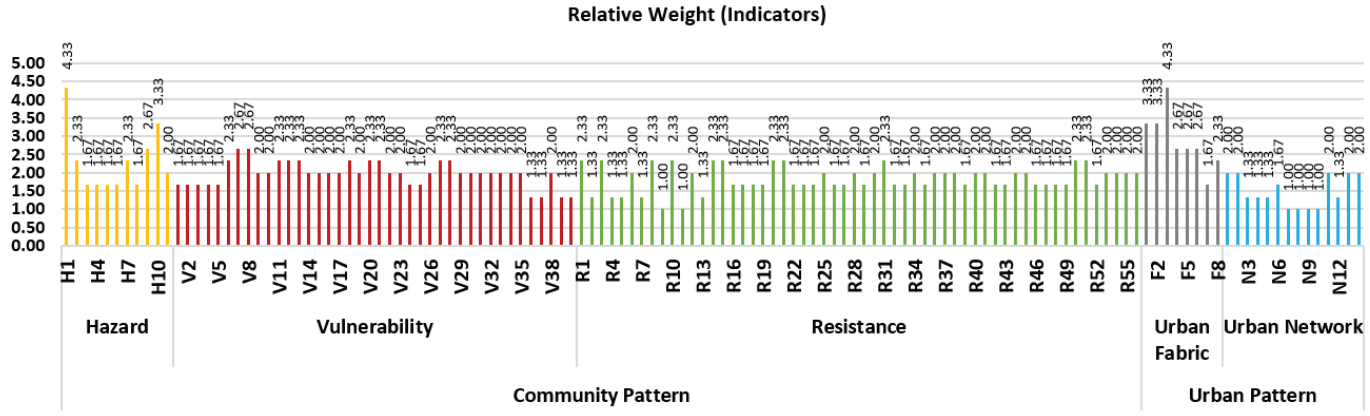


Figure 12: Indicators of UT-NFR and their relative weights.

IV. Discussions

The paper concluded, through inductive research, a framework for the UT-NFR Model depending on the degree of resilience for: (A) urban pattern parameters, and (B) community pattern parameters. Furthermore, the UT-NFR model utilizes a developed mathematical formula that can provide more accurate and realistic measurements in a way that expresses the parameters upon which the Egyptian Urbanism is originally classified.

http://dx.doi.org/10.21622/RESD.2025.11.2.1430

The paper proved that only 58% of the inducted indicators are valid to be included in the final Egyptian UT-NFR model due to:

1. The unavailability of the official data in Egypt, which is still trying to set up a transparent reachable database, has led to exclude a number of non-available indicators from the primary list that deeply express the Egyptian urban context.

2. The uniqueness of the Egyptian urban context compared to the selected global models has led to omitting a number of initial indicators.

3. The instability of the climatic and geological conditions in the eastern Mediterranean zone, where recent non-typical events observed with unusual indicators appeared in the primary list that has been exclusively formulated for this paper.

V. Conclusion

The UT-NFR model is a proposed model that can assess and measure urban resilience against natural flooding risks using two main parameters: (i) the risk of community pattern and (ii) the risk of urban pattern. The model is developed based on the integration of a number of tools, such as "coasts at risk" for assessing community risk, including principles of: (a) hazard, (b) vulnerability, and (c) resistance. Other tools are investigated for assessing the risk of urban patterns, including principles of (d) urban fabric based on a mathematical tool to measure direct or inverse effect on flood damage, and (e) urban network based on a model that measures the survival rate of evacuees during an emergency for an evacuation plan.

A set of indicators is identified representing the main parameters and principles for the Egyptian case, with relative weights determined based on a comparative study highlighting the degree of each global model's reliance on each indicator. Finally, a list of 58% of the proposed indicators is found to be valid for effective inclusion into the final UT-NFR model.

The model is expected to act as a proactive tool to predict urban resilience for new coastal development. Additionally, it can be applied as a reactive tool to assess urban resilience in the existing areas to set up the required contingency preparations by planners and decision-makers.

VI. Future works

The paper introduced a number of research points that may enhance the validity of the proposed UT-NFR model, such as:

1. A field survey investigating the final list of indicators may help in refining and decreasing the number of indicators to increase the applicability and reliability of the tool.

2. Applying the tool on a number of Egyptian coastal areas would definitely help in proving and increasing the validity of the tool; and

3. Applying the tool on other contexts after conducting the required adaptation may help in overcoming a number of natural hazards; especially, in environmental sensitive ecosystems such as rural and desert contexts.

References

[1] S. Bhable, S. N. Kayte, S. Mali, and J. Kayte, "A Review Paper on Coastal Hazard," *Concurr Eng Res Appl*, vol. 5, no. 12, pp. 83–93, 2015.

[2] CRED, "Safer homes, stronger communities : a handbook for reconstruction after natural disaster : Safer homes, stronger communities : a handbook for reconstructing after natural disasters," *Brussels: School of Public Health of the Université Catholique.*, pp. 339–354, 2015.

[3] "Egyptian Ministry of Environment. State of the Environment Report for the Arab Republic of Egypt," *Cairo: Environmental Affairs Agency Publications Office.*, 2017.

[4] M. M. Iskander, "Stability of the Northern coast of Egypt under the effect of urbanization and climate change," *Water Science*, vol. 35, no. 1, pp. 1–10, Jan. 2021, doi: 10.1080/11104929.2020.1864255.

[5] IFRCS, "Road Map to Community Resilience V2. Geneva: International Federation of Red Cross and Red Crescent Societies," 2021.

[6] FEMA, "Resilience Rising; 2024 year in review," *Washington, D.C: U.S Federal Emergency Managment Agency.*, 2025.

[7] UN Habitat, "Trends in Urban Resilience," *Nairobi: UN Habitat*, 2017.

[8] R. Collini *et al.*, "APPLICATION GUIDE for the 2022 Sea Level Rise Technical Report," *National Oceanic and Atmospheric Administration Office for Coastal Management, Mississippi–Alabama Sea Grant Consortium (MASGP-22-028), and Florida Sea Grant (SGEB 88)*, 2022.

[9] "Urban Land Institute , Risk Resilience in Coastal Regions," *Urban Land Institute, Washington DC*, 2013.

[10] S. Gemaila, "The impact of urban form facing tsunami risk," Master's thesis, Faculty of Regional and Urban Planning, Giza, Egypt, 2018.

[11] A. R. Cuthbert, "The Form of Cities," *Oxford: Blackwell Publishing Ltd*, 2006.

[12] E. Mustafa, "Urban typology in Egypt as an introduction to the study of the economics of residential areas," *Giza: Faculty of Regional and Urban Planning, Cairo University*, 1986.

[13] M. R. Berren, A. Beigel, and S. Ghertner, "A typology for the classification of disasters," *Community Ment Health J*, vol. 16, no. 2, pp. 103–111, 1980, doi: 10.1007/BF00778582.

[14] K. H. Eldaimy, "Natural disasters and mitigating their effects," *Cairo: Dar Safaa for Printing, Publishing and Distribution.*, 2013.

[15] J. Hopkins, "Public Health Guide for Emergencies - Disaster Definitions," *Bangladesh: International Federation of Red Cross and Red Crescent Societies*.

[16] L. Chauveau, "Les risques naturels dans le monde. Paris: Larousse Petit atlas des risques écologiques.," 2015.

[17] G. CAMBERS, "COASTAL HAZARDS AND VULNERABLITY," Thesis (Ph.D.), Mayaguez: The University of West Indies., G. Cambers, COASTAL ZONE - ISLAND SYSTEMS MANAGEMENT, 2001.

[18] B. Levin and M. Novos, *Physics of Tsunami*. New York: Springer.

[19] "Egyptian Ministry of Civil Aviation. General Authority of Meteorology," Aug. 2023. [Online]. Available: https://www.civilaviation.gov.eg/Companies/Meteorology#

[20] "Egyptian Authority for Maritime Safety. Seasonal Storms on Egyptian Coasts," 2022. [Online]. Available: https://www.eams.gov.eg/IndexEN

[21] EM-DAT, "Centre for Research on the Epidemiology of Disasters (CRED), from The International Disaster Database (EM-DAT)," 2023. [Online]. Available: https://public.emdat.be/data

[22] A. Z. Hamouda, "A reanalysis of the AD 365 tsunami impact along the Egyptian Mediterranean coast," *Acta Geophysica*, vol. 58, no. 4, pp. 687–704, Aug. 2010, doi: 10.2478/s11600-009-0032-7.

[23] A. I. Okay, O. Tüysüz, and Ş. Kaya, "From transpression to transtension: changes in morphology and structure around a bend on the North Anatolian Fault in the Marmara region," *Tectonophysics*, vol. 391, no. 1–4, pp. 259–282, Oct. 2004, doi: 10.1016/j.tecto.2004.07.016.

[24] H. M. El-barmelgy, "Strategic tsunami hazard analysis and risk assessment planning model : A case study for the city of Alexandria , Egypt," *International journal of development and sustainability*, vol. 3, no. 4, 2014.

[25] M. T. Pareschi, E. Boschi, and M. Favalli, "Holocene tsunamis from Mount Etna and the fate of Israeli Neolithic communities," *Geophys Res Lett*, vol. 34, no. 16, Aug. 2007, doi: 10.1029/2007GL030717.

[26] Wayne and Urlaub, "Upcoming Tsunamis in Mediterranean," *Torino: NEAMTWS*, 2018.

[27] M. Thangaraj, "Potential Threats to Coastal Environment," in *Sustainable Development*, vol. 1, R. G. Bhola, Surampalli Y Rao, and J N Govil, Eds., Studium Press LLC, USA, ch. 9, pp. 208–223.

[28] A. Butt, J. Saleem, I. Zaheer, and A. Jabeen, "Importance of community involvement in coastal area management: A review of International and Pakistani scenario," *International Journal of Biosciences (IJB)*, vol. 12, no. 3, pp. 239–247, Mar. 2018, doi: 10.12692/ijb/12.3.239-247.

[29] A. Masria, A. Negm, M. Iskander, and O. Saavedra, "Coastal Zone Issues: A Case Study (Egypt)," *Procedia Eng*, vol. 70, pp. 1102–1111, 2014, doi: 10.1016/j.proeng.2014.02.122.

[30] M. Depledge, R. Lovell, B. Wheeler, K. Morrissey, M. White, and L. E. Fleming, "Future of the Sea: Health and Wellbeing of Coastal Communities," *London: UK Government Office for Science*, 2017.

[31] R. Bowen, A. Frankic, and M. Davis, "Human Development and Resource Use in the Coastal Zone: Influences on Human Health," *Oceanography*, vol. 19, no. 2, pp. 62–71, Jun. 2006, doi: 10.5670/oceanog.2006.66.

[32] "European Environment Agency. Priority environmental issues in the Mediterranean region. ," *United Nations.Luxembourg: Official Publications Office of the European Union (UNEP).*, 2006.

[33] M. E. Hereher, "Coastal vulnerability assessment for Egypt's Mediterranean coast," *Geomatics, Natural Hazards and Risk*, vol. 6, no. 4, pp. 342–355, May 2015, doi: 10.1080/19475705.2013.845115.

[34] H. Festing, C. Copp, H. Sprague, D. Wolf, B. Shorofsky, and K. Nichols, "The prevalence and cost of urban flooding: A case study of Cook County, IL," *Chicago: The Center For Neighborhood Technology.*, 2014.

[35] "Centers for Disease Control and Prevention (U.S.). Coastal flooding, climate change, and your health what you can do to prepare," *Washington DC: U.S Department of Health and Human Services.*, 2017.

[36] United Nations. Atmospheric and Oceanography Facts. New York: United Nations: The Ocean Conference , 2017.

[37] NASA, "Trending. Retrieved from BBC," Aug. 2019. [Online]. Available: https://www.bbc.com/arabic/trending-50186588

[38] B. L. Valle, N. Kalligeris, A. N. Findikakis, E. A. Okal, L. Melilla, and C. E. Synolakis, "Plausible megathrust tsunamis in the eastern Mediterranean Sea," *Proceedings of the Institution of Civil Engineers - Engineering and Computational Mechanics*, vol. 167, no. 3, pp. 99–105, Sep. 2014, doi: 10.1680/eacm.13.00027.

[39] M. Torab and N. Dalal, "Natural hazards mapping of mega sea waves on the NW coast of Egypt," *Journal of African Earth Sciences*, vol. 112, pp. 353–357, Dec. 2015, doi: 10.1016/j.jafrearsci.2015.09.022.

[40] USAID, "Concepts and Practices of Resilience. Bangkok: U.S. Indian Ocean Tsunami Warning System (IOTWS) Program," 2006.

[41] NOAA, "Coastal Community Resilience Indicators and Rating Systems," *New York: National Oceanographic and Atmospheric Authority*, 2015.

[42] M. Pawlukiewicz, P. K. Gupta, and C. Koelbel, *Ten Principles for Coastal Development*. Washington DC: Urban Land Institute, 2007.

[43] NOAA, "How Resilient Is Your Community," *New York: USAID*, 2007.

[44] M. Caprioli, R. Trizzino, R. Pagliarulo, M. Scarano, F. Mazzone, and A. Scognamiglio, "MANAGEMENT OF ENVIRONMENTAL RISKS IN COASTAL AREAS," *The International Archives of the Photogrammetry, Remote Sensing and Spatial Information Sciences*, vol. XL-3/W3, pp. 263–268, Aug. 2015, doi: 10.5194/isprsarchives-XL-3-W3-263-2015.

[45] S. Hussein, S. Aziz, and R. Nasreldin, "Promoting user well-being in central business district: the role of sustainable open spaces," *Renewable Energy and Sustainable Development*, vol. 10, no. 1, p. 135, May 2024, doi: 10.21622/resd.2024.10.1.827.

[46] Z. Imran and M. Yamao, "Toward Strengthening Social Resilience: A Case Study on Recovery of Capture Fisheries after Asia's Tsunami in Aceh, Indonesia," *World Academy of Science, Engineering and Technology International Journal of Environmental, Chemical, Ecological, Geological and Geophysical Engineering*, vol. 6, no. 9.

[47] J. Gilbert and P. Vellinga, "Coastal Zone Management," *Amsterdam: IPCC Response Strategies Working Group*, pp. 133–160.

[48] J. Preuss, Ed., "Coastal area planning and management with a focus on disaster management and the protective role of coastal forests and trees," in *Coastal Area Planning and Management* , London: the Queenland Government Office., 2005, pp. 133–160.

[49] P. L. Stewart, R. J. Rutherford, H. A. Levy, and J. M. Jackson, "Canadian Technical Report of Fisheries and Aquatic Sciences," *Dartmouth: Bedford Institute of Oceanography*, 2003.

[50] M. A. Esmat, A. Ahmed, E. Othman, H. Elsaay, and T. Haupt, "Strategic Crisis Management in Egypt in: An investigation on the role of resilient design in mitigating the impacts of coastal floods," 2019.

[51] NOAA, "Achieving Hazard-Resilient Coastal & Waterfront Smart Growth," *Washington DC: U.S. Environmental Protection Agency*, 2020.

[52] "HM Government. Evacuation and Shelter Guidance," *York: Easingwold Publishing*, 2006.

[53] N. Azouz, M. A. Khalifa, and M. El-Fayoumi, "Mobility inequality of disadvantaged groups in Greater Cairo region," *Renewable Energy and Sustainable Development*, vol. 10, no. 1, p. 1, Feb. 2024, doi: 10.21622/resd.2024.10.1.753.

[54] S. Scheer *et al.*, "Tsunami Evacuation Planning," *Luxembourg: The European Union*, 2011.

[55] E. Neron, F. Audin, I. Ndiaye, K. Boukebab, K. Serrhini, and M. Maizia, "Decision Support System for Large-Scale Evacuation Logistics," *Nice: The National Research Agency of France*, 2012.

[56] C. Duffy, "Tsunami notification process plan. Alaska: Province of British Colombia," 2013.

[57] L. R. Santibáñez, "Urban Evacuation Tsunamis: Guidelines for Urban Design," *Journal of Engineering and Architecture*, vol. 4, no. 2, 2016, doi: 10.15640/jea.v4n2a10.

[58] M. Jenks, "City Form: The Sustainable Urban Form Consortium," *Journal of Architectural/ Planning Research and Studies (JARS)*, vol. 4, pp. 89–102, Oct. 2006, doi: 10.56261/jars.v4.169188.

[59] Y. R. Jabareen, "Sustainable Urban Forms," *J Plan Educ Res*, vol. 26, no. 1, pp. 38–52, Sep. 2006, doi: 10.1177/0739456X05285119.

[60] A. Sharifi, "Urban Resilience Assessment: Mapping Knowledge Structure and Trends," *Sustainability*, vol. 12, no. 15, p. 5918, Jul. 2020, doi: 10.3390/su12155918.

[61] J. Hewitt, R. Potangaroa, and S. Wilkinson, "The role of urban change hierarchies in post-disaster recovery," *Building resilience*, pp. 1–11, 2008.

[62] T. K. Jha, A. , W. Miner, and Z. S. Geddes, "Building Urban Resilience. Australian AID," *Washington DC: The World Bank*, 2013.

[63] K. Wiliams, "Urban Form and Infrastructure: A morphological review," *Bristol: Foresight, United Kingdom Government Office for Science*, 2014.

[64] "Human Settlements Program. Rapid Urban Planning Tools For City Extension : Urban Typologies," *United Nations, UN Habitat. Nairobi: UN Habitat*, 2014.

[65] A. A. Hemida, M. A. E. Khalifa, M. Abdelsalheen, and S. Afifi, "Coastal vulnerability assessment in urban planning: a comparative tool-based selection approach for the Egyptian context," *Renewable Energy and Sustainable Development*, vol. 10, no. 1, p. 32, Mar. 2024, doi: 10.21622/resd.2024.10.1.755.

[66] Q. Yang, Y. Sun, X. Liu, and J. Wang, "MAS-Based Evacuation Simulation of an Urban Community during an Urban Rainstorm Disaster in China," *Sustainability*, vol. 12, no. 2, p. 546, Jan. 2020, doi: 10.3390/su12020546.

[67] Y. Zhu, K. Xie, K. Ozbay, and H. Yang, "Hurricane Evacuation Modeling Using Behavior Models and Scenario-Driven Agent-based Simulations," *Procedia Comput Sci*, vol. 130, pp. 836–843, 2018, doi: 10.1016/j.procs.2018.04.074.

[68] H. Yang, E. F. Morgul, K. Ozbay, and K. Xie, "Modeling Evacuation Behavior Under Hurricane Conditions," *Transportation Research Record: Journal of the Transportation Research Board*, vol. 2599, no. 1, pp. 63–69, Jan. 2016, doi: 10.3141/2599-08.

[69] K. Clifton, R. Ewing, G. Knaap, and Y. Song, "Quantitative analysis of urban form: a multidisciplinary review," *Journal of Urbanism: International Research on Placemaking and Urban Sustainability*, vol. 1, no. 1, pp. 17–45, Mar. 2008, doi: 10.1080/17549170801903496.

[70] S. Kang, J. Yeom, and J. Jung, "Urban Form and Natural Hazards: Exploring the Dual Aspect Concept of Urban Forms on Flood Damage," *Sustainability*, vol. 13, no. 16, p. 9007, Aug. 2021, doi: 10.3390/su13169007.

[71] M. W. Beck, "Coasts at Risk: An Assessment of Coastal Risks," *Rhode Island: United States Agency for International Development (USAID)*, 2014.

[72] A. Tragaki, C. Gallousi, and E. Karymbalis, "Coastal Hazard Vulnerability Assessment Based on Geomorphic, Oceanographic and Demographic Parameters: The Case of the Peloponnese (Southern Greece)," *Land (Basel)*, vol. 7, no. 2, p. 56, May 2018, doi: 10.3390/land7020056.

[73] G. Brunetta and S. Salata, "Mapping Urban Resilience for Spatial Planning—A First Attempt to Measure the Vulnerability of the System," *Sustainability*, vol. 11, no. 8, p. 2331, Apr. 2019, doi: 10.3390/su11082331.

[74] D. Rogers and V. Tsirkunov, *Costs & Benefits of Early Warning*. Moscow: The World Bank., 2010.

[75] J. M. Jones, P. Ng, and N. J. Wood, "The Pedestrian Evacuation Analyst: geographic information systems software for modeling hazard evacuation potential," 2014. doi: 10.3133/tm11C9.

[76] M. Yehia, Y. Kandil, and N. A. Fouad, "Understanding walkability criteria in high-density communities: a case study in Alexandria, Egypt," *Renewable Energy and Sustainable Development*, vol. 10, no. 1, p. 169, Jun. 2024, doi: 10.21622/resd.2024.10.1.799.